Stabilization of Al(III) solutions by complexation with cacodylic acid: speciation and binding features

Matteo Lari[a], Héctor Lozano[a], Natalia Busto[a], Tarita Biver[b], José M. Leal[a], Saturnino Ibeas, [a] James A. Platts[c], Fernando Secco[b], Begoña Garcia[a]*.

[a] *Departamento de Química, Universidad de Burgos, Plaza Misael Bañuelos s/n, 09001 Burgos, Spain*
[b] *Dipartimento di Chimica e Chimica Industriale, Università di Pisa, Via Moruzzi 13, 56124 Pisa, Italy*
[c] *School of Chemistry, Cardiff University, Park Place, Cardiff CF10 3AT, UK.*
*Corresponding author: begar @ubu.es

Abstract Aluminium ion is thought to cause a variety of neurological and skeletal disorders in man. The study of the biological processes and molecular mechanisms that underlie these pathological processes is made difficult because of the complexity of species resulting from the hydrolysis of Al^{3+} ion. In addition, this ion displays a strong tendency to precipitate as hydroxide. so that certain complexing agents should be envisaged in order to stabilize solutions of Al(III) under physiological conditions. In this work, we show that the common buffer cacodylic acid (dimethylarsinic acid, HCac) interacts with Al(III) to give stable complexes, even at pH 7. After preliminary analyses of the speciation of the metal ion and also of the ligands, a systematic study of the formation of different Al/Cac complexes at different pH values has been conducted. UV-Vis titrations, mass spectrometry and NMR measurements were performed to enlighten the details of the speciation and stoichiometry of Al/Cac complexes. The results altogether show that Al/Cac dimer complexes prevail, but monomer and trimer forms are also present. Interestingly, it was found that cacodylate promotes the formation of such relatively simple complexes, even under conditions where the polymeric form, $Al_{13}O_4(OH)_{24}^{7+}$, should predominate. The results obtained can be useful to study the reactivity of aluminium ion in the biological environment.

Keywords: Aluminium complexes, dimethylarsinic acid, Al(III) speciation, ^{27}Al-NMR.

1. Introduction

Aluminium ion is prone to forming a variety of hydrolytic species,[1] including the $Al_{13}O_4(OH)_{24}^{7+}$ polymeric form; it exhibits certain tendency to precipitate as $Al(OH)_3$ even at relatively acidic pH, and reacts with oxygen-containing ligands.[2,3] Many studies have enlightened the importance of aluminium in biological fluids and its ability to bind biosubstrates, both outside and inside the cell, associating its presence to health diseases.[4-8] The presence of different hydrolytic forms entails involvement of a number of equilibria and, consequently, many other possible complexes. These features render aluminium a very complex system.

Dimethylarsinic (cacodylic) acid, $(CH_3)_2AsOOH$, is largely used to study the interaction of biological molecules with organic dyes or metal ions.[9] Cacodylic acid (HCac, pK_A = 6.2 0.1), with a buffer window ranging pH 5.2 - 7.2,[10-13] is quite a valuable tool to study nucleic acids and proteins under physiological conditions. On the other side, the cacodylate anion is unreactive towards many divalent metal ions;[14] for this reason it is thought to ensure buffer inactivity for many biomolecule/metal ion (or metal complex) systems. On the other hand, there is evidence that the cacodylate anion can bind metal ions such as Sb(III), Bi(III),[15] Pd(II)[16] and some rare earth metals.[17] Formation of Al(III)/Cac complex[18] and, more recently, the synthesis of complexes of the dimethylarsinate anion and metal ions of the XIII group (Al, Ga, In, Tl) has been

reported.[19] However, to the best of our knowledge, systematic thermodynamic studies of the aluminium/cacodylic acid system in solution under different experimental conditions are still lacking. This work focuses on the study of the Al(III)/Cac system at different pH values to infer the nature and strength of the interaction between Al(III) and the ligand and to assess the possible use of cacodylate to provide Al(III) buffered solutions for biochemical studies at neutral pH.

2. Materials and Method

2.1. Materials

The aluminium source was the $Al(ClO_4)_3 \cdot 8H_2O$ solid salt supplied by Fluka. Aluminium stock solutions were prepared by dissolving appropriate amounts of the solid in $HClO_4$ solutions, brought at pH = 2 to avoid hydroxide precipitation. The standardization of aluminium stock solutions was carried out through EDTA titrations, using Eriochrome Black-T as an indicator. Briefly, a calibrated excess of EDTA was added to an aliquot of the aluminium solution; the mixture was then boiled and, after addition of acetate buffer (pH = 6), it was back titrated with a standardized solution of Zn^{2+}. Stock solutions of sodium dimethylarsinate ($(CH_3)_2AsOONa$, NaCac - Carlo Erba, purity 96%) were prepared by dissolving weighed amounts of the solid in water and titrated with NaOH. The ionic strength (I) of the working solutions was kept constant at 0.1 M with sodium perchlorate (Merck), while the desired pH was attained by small additions of NaOH and $HClO_4$. All of the reactants were analytical grade and were used without further purification. Ultra-pure water from a Millipore MILLI-Q water purification system was used to prepare the solutions and as a reaction medium.

2.2. Methods

pH measurements were performed with a Metrohm 713 (Herisau, Switzerland) pH-meter equipped with a combined glass electrode. Spectrophotometric titrations were carried out with a Shimadzu 2450-Spectrophotometer, equipped with jacketed cell holders (thermostat precision 0.1 °C). All experiments were conducted at 25 °C. Titrations of Al(III)/Cac system were performed in the batch-wise mode at the desired pH values and ionic strength 0.1 M ($NaClO_4$). Different samples were prepared for different metal-to-ligand ratio and left for 24 h to reach equilibration. For each sample, the absorbance spectrum was recorded in the 190-300 nm range (path-length cell 1 cm) and the binding parameters were evaluated averaging the results obtained at different selected wavelengths in the 205-193 nm range. Mass spectra in double distilled water recorded for samples at $C_L/C_M = 1$ ($C_M = 0.2$ mM), C_L and C_M being, respectively, the cacodylate and aluminium ion concentrations, were obtained by means of a TOF Mass Spectrometer Bruker Maxis Impact, with electrospray ionization (ESI). NMR samples were prepared by dissolving in 0.5 mL of the respective oxygen-free deuterated solvent the proper amount of Al^{3+} to 5 mM working solutions with the corresponding amount of Sodium Cacodylate for each C_L/C_M ratio studied. Unless otherwise stated, the spectra were recorded at 298 K on a Varian Unity Inova-400 (399.94 MHz for ^{1}H; 104.21 MHz for ^{27}Al). Typically, 1D ^{1}H NMR spectra were acquired with 32 scans into 32 k data points over 16 ppm spectral width; the spectra of ^{27}Al NMR were acquired with 16 scans. ^{1}H chemical shifts were referenced internally to TMS via 1,4-dioxane in D_2O ($\delta = 3.75$ ppm). Chemical shift values are reported in ppm. All of the NMR data processing were carried out using MestReNova version 6.1.1.

DFT calculations were carried out using B3LYP functional to optimize some proposed structures for the aluminium-sodium cacodylate complex; this procedure was used satisfactorily for DFT calculations of metals,{Lashkari, 2004, DFT studies of pyridine corrosion inhibitors in electrical double layer: solvent`, substrate`, and electric field effects}[20] applying 6-31G(d) basis set to C, H and O atoms. A double zeta function (LANL2DZ) was used for Al and As, including effective core potential calculation (ECP) for core electrons, diminishing the computational calculation costs. Water was used as solvent. All calculations and data analyses were performed with Gaussian 09.[21]

3. Results and Discussion

3.1. Evaluation of the $pK_{A,1}$ and $pK_{A,2}$ acidity constants of cacodylic acid

Cacodylic acid is a diprotic acid; its diprotonated form is here denoted as H_2Cac^+. This species undergoes acid dissociation according to eqns (1) and (2), which are characterized by the acid dissociation constants $K_{A,1}$ and $K_{A,2}$ respectively.

$$H_2Cac^+ + H_2O \rightleftarrows HCac + H_3O^+ \quad (1)$$

$$HCac + H_2O \rightleftarrows Cac^- + H_3O^+ \quad (2)$$

The ^{1}H-NMR spectra of cacodylate shows a singlet signal ascribable to the methyl groups of NaCac. The location of these peaks very much depends on the medium acidity for the higher acidity, the higher the chemical shift of the peaks (Fig.

1A).

The $pK_{A,1}$ and $pK_{A,2}$ values have been determined by the chemical shift analysis of the ^{1}H-NMR singlets of sodium cacodylate at different values of the pH and the acidity function H_0 (Fig. 1B); the latter function was employed at the highest acidity levels used, outside the boundary of the pH scale.[22] The two dissociation constants of cacodylic acid were evaluated according to eqn (3):

(3)

where $_B$ and $_{BH+}$ represent the chemical shift of the basic and acidic forms, respectively, and that at an intermediate acid concentration, according to species shown in eqns. (1) and (2). The chemical shift of the basic form ($_B$) at pH = 8 is not well defined, thereby to evaluate $_B$ and $pK_{A,2}$ an iteration procedure had to be used. To determine $pK_{A,1}$, eqn. (3) was applied directly by adopting for $_B$ the chemical shift at pH = 4, whereas that for $_{BH+}$ was taken as the highest value in Fig. 1B. The continuous line denotes the outcome of the two fittings. The $pK_{A,1}$ and $pK_{A,2}$ values obtained, 1.3 0.2 and 6.2 0.1 respectively, were in reasonable good agreement with the literature values, $pK_{A,1}$ = 1.1[10] and 2.6[23], and $pK_{A,2}$ = 6.2[10-13]. Fig. 1C shows the speciation curves of cacodylic acid.

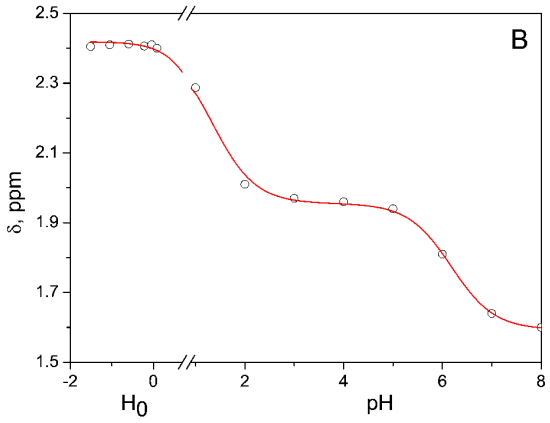
B
δ, ppm
2.5
2.3
2.1
1.9
1.7
1.5
-2
0
2
4
6
8
H0
pH

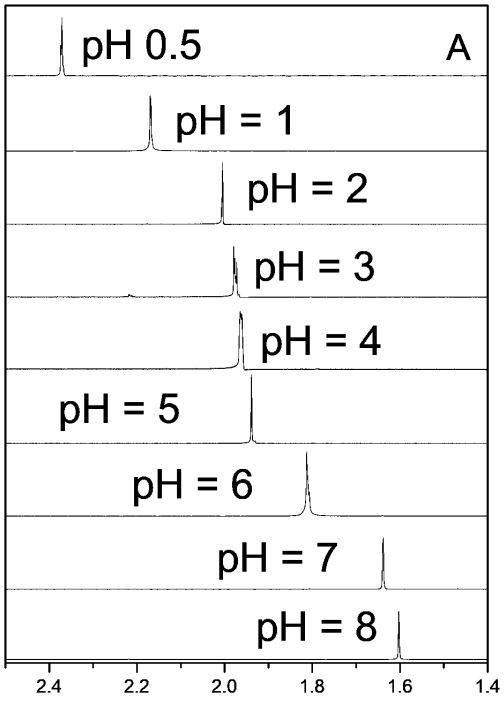
pH 0.5
A
pH = 1
pH = 2
pH = 3
pH = 4
pH = 5
pH = 6
pH = 7
pH = 8
2.4
2.2
2.0
1.8
1.6
1.4
δ, ppm

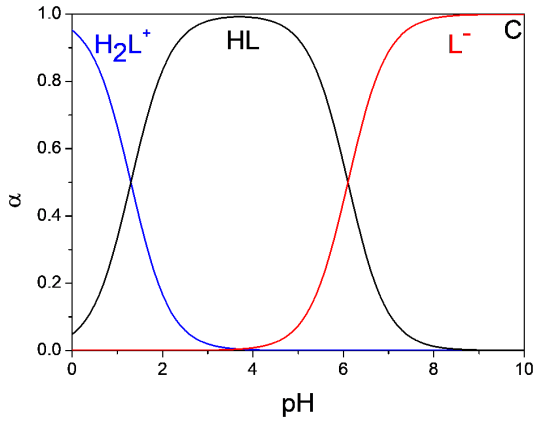

Fig. 1 (A) ^{1}H-NMR spectra at pH= 0.5, 1, 2, 3, 4, 5, 6, 7 and 8. (B) δ versus pH (or H_0) plot corresponding to $pK_{A,1}$ and $pK_{A,2}$. $C_L = 5.00 \times 10^{-3}$ M. (C) Speciation of cacodylic acid ($pK_{A,1}$ = 1.3, $pK_{A,2}$ = 6.1). I = 0.1 M ($NaClO_4$), T = 25.0 °C.

As for the absorbance measurements, Fig. S1 (ESI) shows the spectra of cacodylic acid at different pH values (I = 0.1 M, $NaClO_4$). The change in absorbance

upon titration within the 2-10 pH range (Fig. S1, inset) has enabled us to evaluate the second acid dissociation constant of cacodylic acid, the resulting value being: $pK_{A,2}$ = 6.0 ± 0.2. Below pH 3, the shift of the 193 nm band to lower wavelengths can be ascribed to formation of the H_2Cac^+ species.

3.2 Speciation of aluminium forms

Fig. 2 shows the ^{27}Al-NMR spectra in the 1–6 pH range (above pH 6 the measurements could not be executed because aluminium precipitates). NMR measurements show that the hexaaquoaluminium(III) ion, $Al(OH)_6^{3+}$, prevails between pH 1 and 4. The wide band in ^{27}Al-NMR spectra observed between pH 5 and 6 can be ascribed to the polycation species $Al_{13}O_4(OH)_{24}^{7+}$ (also denoted as Al_{13}-mer).[24] Between pH 6 and 7, partial or full neutralization of the polymer charge promotes aggregation of Al_{13}-mer, which tends to precipitate, and formation of more complex polymeric forms, such as $Al_2O_8Al_{28}(OH)_{56}(H_2O)_{26}^{18+}$ (also known as Al_{30}-mers) is likely to occur.[25,26]

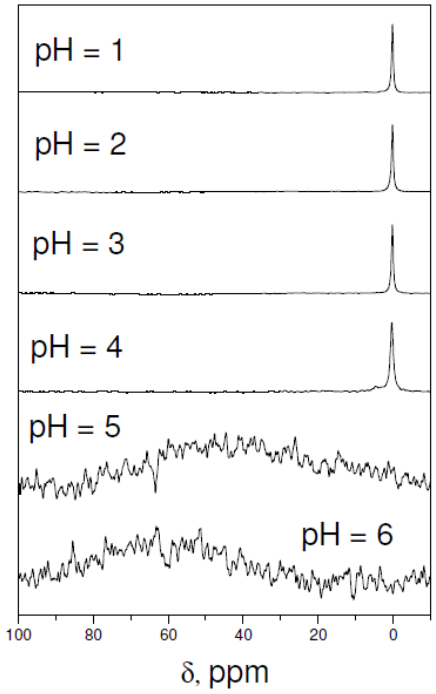

Fig. 2 ^{27}Al-NMR spectra of Al(III) at different pH values. $C_M = 5.00 \times 10^{-3}$ M, I = 0.1 M ($NaClO_4$) and T = 25.0 °C. The pH-independent narrow peak at δ (roughly) 0 ppm, is ascribed to the monomeric species Al^{3+}, whereas the broad band observed at pH 5 and 6 is the $Al_{13}O_4(OH)_{24}^{7+}$ polymer.

The NMR findings are corroborated by literature data. The molar fraction (β)

of the Al^{3+} hexahydrate ion and its hydrolytic forms can be calculated according to eqn (4):[1]

(4)

where I is the ionic strength of the medium, Q_{xy} is the equilibrium ratio related to formation of the hydrolyzed $Al_x(OH)_y^{(3x-y)+}$ species ($xAl + yH_2O \rightleftharpoons Al_x(OH)_y^{(3x-y)+} + yH^+$) and K_{xy} is the relevant thermodynamic equilibrium constant, ***a*** and ***b*** being fitting parameters and m_x is the overall aluminium molality.[1] This calculation was performed at different pH values and metal concentrations using the Octave program,[27] yielding the distribution plots shown in Fig. 3. This figure shows that the amount of dimer and trimer species is negligible and that the predominant species in the 4.5 to 8.0 pH range is $Al_{13}O_4(OH)_{24}^{7+}$ whereas $Al(OH)_4^-$ is the prevailing species above pH 8.

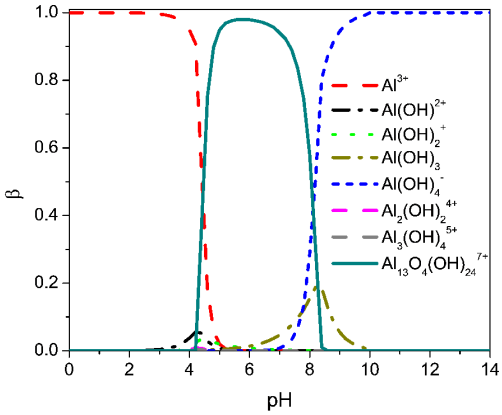

Fig. 3 Speciation of Al(III). $C_M = 1.00 \times 10^{-3}$ M, I = 0.1 M and T = 25.0 °C.

The results from Fig. 3 are compared in Fig. S2 (A and B, ESI) with other results obtained for Al^{3+} concentrations of 1.0×10^{-4} and 1.0×10^{-5} M, showing that polymeric species are absent in dilute solutions. Additionally, an increase in the aluminium concentration (C_M) causes a small diminution of $\beta_{Al^{3+}}$ and a sharp increase of the polymeric form $Al_{13}O_4(OH)_{24}^{7+}$.

3.3. The aluminium/cacodylate system

Mass spectrometry. The different number of peaks recorded at different pH reveals the complexity of the distribution of the aluminium species (Fig. S3, ESI). We

focused the attention on the most representative peaks in the spectrum and determined four types of species: **(1)** free cacodylate, which is predominant and in particular the $[HCac + H]^+$ (m/z = 139) and $[NaCac + H]^+$ (m/z = 161) adducts and other peaks reported in literature,[28, 29] such as m/z = 277, 259, 299, 281, 437 and 419 (corresponding to $[H_2Cac_2+H]^+$, $[H_2Cac_2+H-H_2O]^+$, $[H_2Cac_2+Na]^+$, $[H_2Cac_2+Na-H_2O]^+$, $[H_3Cac_3+Na]^+$, $[H_3Cac_3+Na-H_2O]^+$), respectively; **(2)** perchlorate and cacodylate salt clusters: $[Na(NaClO_4)_x]^+$ (m/z = 145, 267, 389) and $[Na(NaCac)_x]$ (m/z = 183, 343, 503, 663); **(3)** Al uncomplexed forms: $Al(OH)_2(H_2O)_v^+$ (m/z = 79, 115, 133); $Al_2O(OH_2)_3^+$ (m/z = 121) and **(4)** Al/Cac complexes. By analogy with the formulation of aluminium(III) of aquo-chloro-complexes, we adopt the general formula $Al_xO_y(OH)_zCac_u(H_2O)_v^{n+}$ for the aluminium/cacodylate complexes.[30] The distribution of the different forms is shown in Fig. 4, whereas the respective formulas are summarized in the Electronic Supporting Information (Table 1 ESI).

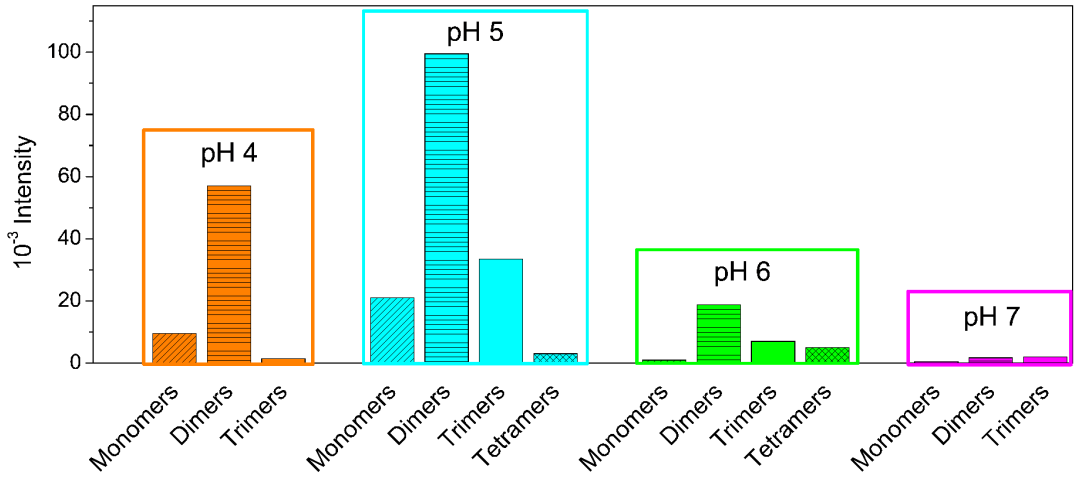

Fig. 4 Distribution of the different forms of Al/Cac complexes at different pHs. $C_L = C_M = 2.00 \times 10^{-4}$ M and T = 25.0 °C.

However, it should be pointed out here that assignment of the proper formula is prone to ambiguity.[31] In the first place, the $(OH)_2^{2-}$ and $O(OH_2)^{2-}$ patterns, having the same value of the m/z ratio, cannot be differentiated. Therefore, $Al_2O(OH)Cac_2(H_2O)^+$ could be replaced by $Al_2(OH)_3Cac_2^+$. Moreover, some peaks can be assigned to either a free or a bound aluminium species. For instance, the peak at m/z = 121 can be ascribed to the free species $Al_2O(OH)_3^+$ and to the $Al_2O(OH)Cac(H_2O)_v^{2+}$

complex, and the peaks at 301 and 319 to the 1:2 complex $AlCac_2(H_2O)_v^+$ or to the 3:1 $Al_3O(OH)Cac(H_2O)_v^+$ complex. The theoretical (see below) and literature[30-34] data will allow us to suggest the most stable form.

At pH 4, 5 and 6 the most intense peaks are those associable to the dimeric forms. On the other hand, monomeric species are mainly present not only at pH 5, but also at pH 4. Trimeric forms display lower intensity signals and are detected at pH 5, 6 and 7. In particular, the signal at pH 7 is lower than those detected at pH 5 and 6, concurrent with the weakening of the interaction of cacodylate at neutral pH, observed in the NMR experiments as described below.

The high abundance of dimeric complexes contrasts with the β values, indicating rather modest presence of dimers when cacodylate is absent (Fig. 3). To support this view, previous studies[30-34] on aluminium complexes with organic ligands have shown that $Al_2O(OH)_3^+$ yields a small peak, suggesting that the dimeric aluminium free species are only poorly present in solution. Hence, it can be surmised that the presence of cacodylate induces, in addition to the 1:1 complex , the formation of ligand bound dimeric and (to a lesser extent) also trimeric and tetrameric species. Furthermore, the fact that the peaks of these species are present also at pH 5 and 6, where, in the absence of ligand, the polymeric form Al_{13}-mer is far prevailing, suggests that the ligand induces the disintegration of Al_{13}-mer to give smaller molecules.

^{27}Al-NMR and ^{1}H-NMR studies. Fig. 5A shows the ^{27}Al-NMR spectra for Al/Cac in the pH 1 – 7 range. Between pH 1 and 2, only the signal corresponding to free Al^{3+} was observed at 0 ppm. In addition to the signal at 0 ppm, at pH 3 and 4, two further signals, at 2 and 4 ppm, were observed, the former remaining very modest at the two pH values. The second displays a remarkable increase in intensity on going

from pH 3 to pH 4. At pH 5 and 6, a wide band is observed at 8 and 12 ppm, respectively. At pH 7, the centre of the band is shifted to 60 ppm.

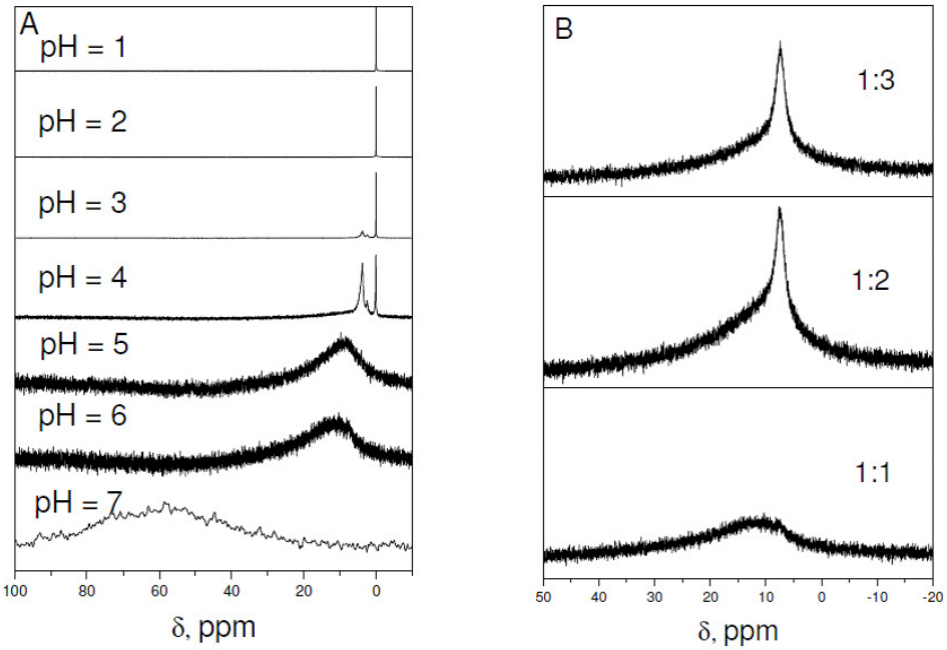

Fig. 5 ^{27}Al-NMR spectra for (A) Al/NaCac system at pH = 1, 2, 3, 4, 5, 6 and 7, C_M/C_L = 1:1 (B) Al/NaCac system at C_M/C_L = 1:1, 1:2 and 1:3, $C_M = 5.00 \times 10^{-3}$ M, pH = 6.0, I = 0.1 M ($NaClO_4$) and T = 25 ºC.

Fig. 6 shows the ^{1}H-NMR spectra of the Al/NaCac system recorded at different pH values and different times. The peak of the free ligand (circled), and other peaks are displayed in the 4 pH 7 range, which are associated to the bound cacodylate. The whole of the ^{27}Al-NMR and ^{1}H-NMR experiments have contributed to interpret the behaviour of the aluminium/cacodylate system at different pH values.

t = 10 min

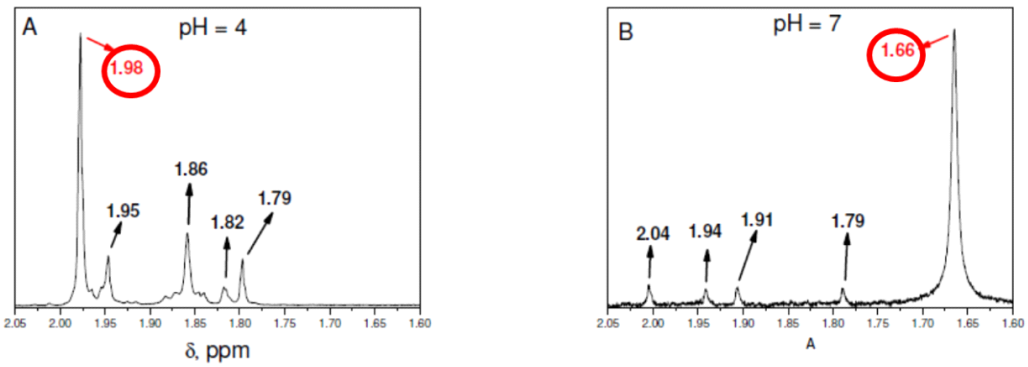

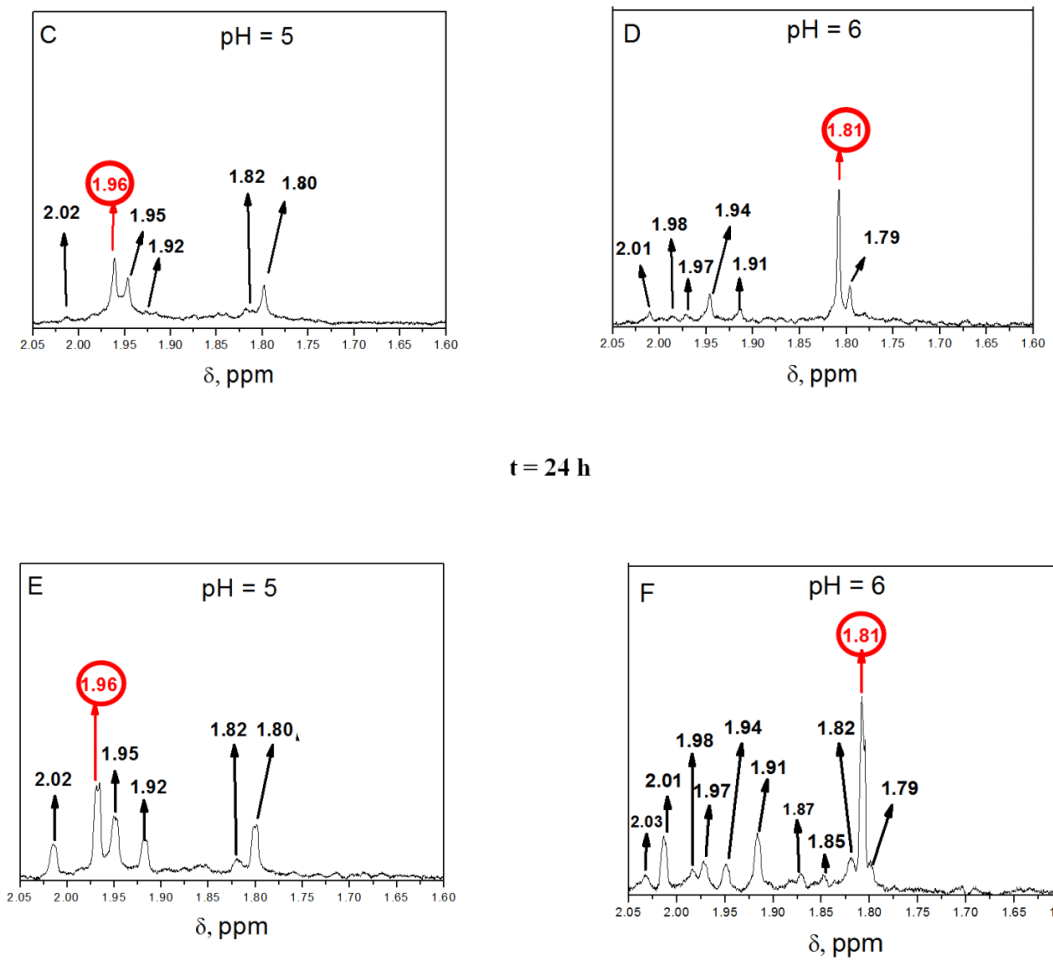

Fig. 6 ^{1}H-NMR kinetics of Al/NaCaC complex at t = 10 min (A, B, C and D) and t = 1 day (E and F). $C_M = C_L = 5.00 \times 10^{-3}$ M, I = 0.1 M ($NaClO_4$), pH = 4–7 and T = 25 °C. Circled chemical shift stands for free cacodylate at every pH.

No Al/Cac complex is formed at pH 1 and 2. However little amounts of complex are detected at pH 3 and the extent of binding becomes more and more important as the pH is raised, in agreement with the general behaviour displayed by complex formation reactions of metal ions with ligands protonated at the reaction site.

Concerning the data at pH 4, comparison of the ^{27}Al-NMR spectra of free (Fig. 2) and bound (Fig. 5A) aluminium shows a remarkable increase of the peak at 4 ppm,

which can be associated to the dimeric aluminium/cacodilate form.[35,36] In the ^{1}H-NMR spectrum (Fig. 6A), the singlet at 1.86 can be associated to the monomeric $AlCac^{2+}$ form, since δ = 1.86 ppm is associated to the Al^{3+} ion according to the data of Fig. 5A. The two peaks at 1.95 and 1.79, having the same intensity, most likely correspond to a dimeric form, in which the two methyl groups have different environment. Also other small peaks are present, in particular in the 1.88-1.85 ppm range and at 1.82 ppm, which can be related to other monomeric species, such as $Al(OH)Cac^{+}$.

The broad peak observed at pH 5 and 6 in the ^{27}Al-NMR experiments (Fig. 5A) should be associated to the sum of dimeric, trimeric and other polymeric species coming from the decomposition of the Al_{13} aggregate associated to the broad peak at 60 ppm (Fig. 2). In addition, ^{27}Al-NMR spectra recorded at pH 6 for C_L/C_M 1, 2 and 3 show constriction of the broad peak, with signal increase at 7.5 ppm (Fig. 5B). This behaviour agrees well with further disintegration of the Al_{13}-mer in the presence of an excess of cacodylate. The ^{1}H-NMR experiments show that the peak at 1.86 ppm, present at pH 4, disappears when the solution pH is raised (spectra at pH 5 and 6 in Figs. 6C and 6D), while the peaks at 1.95 and 1.80 ppm exhibit remarkable intensity. Moreover, a very slow kinetic process is observed, followed by the increase of two peaks at 2.01 and 1.92 ppm, of same intensity (Figs. 6E and 6F). Therefore, we can surmise that the interaction between aluminium and cacodylate is the summation of two reactions. The first one is fast, possibly representing the ligand binding to monomeric or dimeric aluminium species and the second represents the decomposition of the polymeric Al_{13}-mer induced by the interaction of cacodylate to give simpler species, in agreement with the observed disaggregation of Al_{13}-mer induced by ligands with oxygen containing groups, such as acetate, oxalate and lactate and, more

conceivably, by protons.[26,37-39] In this case, disaggregation seems to be strongly dependent on the pH and less on the ligand.

Furrer et al[37] state that the disaggregation of Al_{13}-mer is driven by the proton concentration. In other words, the only presence of cacodylate does not allow by itself the disaggregation of the aluminium oligomers under the experimental conditions (C_L/C_M = 1). However, ^{1}H NMR spectra (Fig. S4, ESI) show that excess of ligand causes an increase in the peak intensity associated to the complexed cacodylate. Thus, some competition between the inner and outer coordination spheres can be guessed in excess of ligand, where the first one can evolve to simpler forms by disruption of the polymer.

The results at pH 7 significantly differ from the trend observed at pH 5 and 6. A very broad, low intensity, peak centred at 60 ppm is obtained in ^{27}Al-NMR spectra (Fig. 5A), and the ^{1}H-NMR exhibits very small peaks of the complexed forms (Fig. 6B), even at same resonance of the peaks at pH 5 and 6. However, at pH 7 no precipitation was observed in the Al/Cac solution, whereas extended precipitation occurs for the free aluminium. Thus, we can envisage occurrence of interaction, even though of different nature compared to that at work at lower pH values.

Stumm[40] suggested that the interaction of an organic ligand with a solid interface can be differentiated between inner (strong bonding) and outer (weak bonding) coordination sphere. In a study of the acetate/aluminium system[41] it has been proposed that the interaction of the acetate ion with Al_2O_3 in suspension involves mainly the outer coordination sphere.[37] We suggest that at pH 7 cacodylate can interact with Al(III) aggregates in the same way as acetate reacts with aluminium oxide

suspension. The resulting complex enables aluminium to remain in solution.

Determination of K_{app} of aluminium/cacodylate complexes. The apparent equilibrium constant, K_{app}, for formation of the aluminium/cacodylate (Al/Cac) complexes, was determined from batch-wise spectrophotometric titrations performed for different pH values. The apparent reaction is

$$M_f + L_f \rightleftharpoons ML_T \qquad (5)$$

where M_f and L_f are respectively the non-complexed free metal and the ligand forms, and ML_T is the total complex. Most of the experimental data-pairs were obtained with no excess of metal or ligand. The interaction between aluminium species and cacodylate causes a hypochromic effect (Fig. 7A). The data-pairs were analysed according to eqn. (6):

(6)

where C_L and C_M are the analytical ligand and metal concentration, respectively, $\Delta A = A-\varepsilon_L C_L$ and $\Delta\varepsilon = \varepsilon_{ML}-\varepsilon_L$, where ε_i is the absorptivity of the i^{th} species.

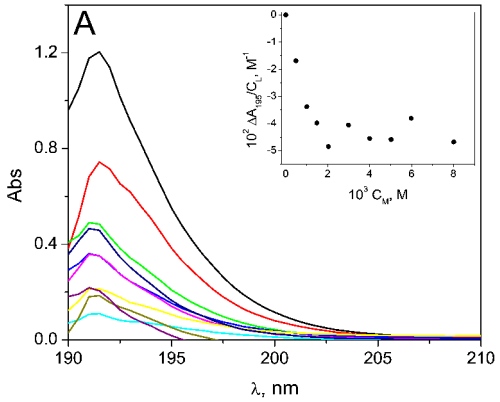
A
1.2
0.8
0.4
0.0
Abs
190
195
200
205
210
λ, nm
0
-1
-2
-3
-4
-5
$10^2 \Delta A_{195}/C_L$, M^{-1}
0
2
4
6
8
10^3 C_M, M

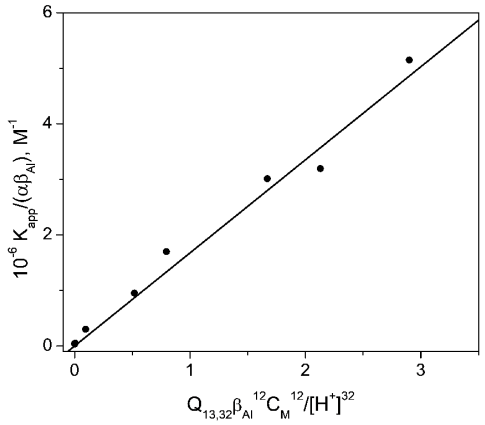

Fig. 7 (A) Example of spectrophotometric titration of the Al/Cac system. Inset: track at λ = 195 nm. $C_L = 1.0 \times 10^{-3}$ M, I = 0.1 M, pH = 4.8 and T = 25.0 °C. (B) Analysis according to eqn (8) of the 4.3 < pH < 5.0 data.

Different binding isotherms were obtained using absorbance values within 195-205 nm (Fig. 7A), a range where aluminium ion displays no absorption, whereas the different dimethylarsinic forms have different absorptivity, ε_i. The equilibrium constants obtained (Table 1) are averaged values. At pH = 2, such evaluation was unfeasible because the change in absorbance was too modest owing to the repression of the binding reaction caused by protons, and in agreement with the NMR results.

Table 1. Apparent equilibrium constant for binding of aluminium to cacodylate (K_{app}) at different pH. I = 0.1 M and T = 25 °C.

pH	K_{app} (M^{-1})
3.00	25±5
4.00	290±50
4.30	560±60
4.48	2200±300
4.70	3400±600
4.78	4600±900
4.90	5400±1000
4.95	4800±1000
5.00	6500±1000

The relationship between K_{app}, and $[H^+]$ is expressed by eqn (7) (see ESI)

(7)

where α_L is the molar fraction of the species Cac^-, β_{Al} is the molar fraction of the species Al^{3+}, K^I, K^{II}, K^{III}, K^{IV}, K^V, K^{VI}, K^{VII} and K^{VIII} are the equilibrium constants for binding of Cac to Al^{3+}, $Al(OH)^{2+}$, $Al(OH)_2^+$, $Al(OH)_3$, $Al(OH)_4^-$, $Al_2(OH)_2^{4+}$, $Al_3(OH)_4^{5+}$ and $Al_{13}O_4(OH)_{24}^{7+}$, respectively. On the other side, the values (Fig. 3) support simplification of eqn (7) to eqn (8). In fact, all contributions, except those of Al^{3+} and Al_{13}-mer, are negligible for, under the employed experimental conditions, the mole fraction of the other species is low.

(8)

Moreover, since formation of the polymeric form is fully attained within a very narrow pH range, two well defined pH ranges can be distinguished; in the first ($3.0 < pH < 4.3$) the monomers Al^{3+} and $AlOH^{2+}$ are active, while in the second ($4.7 < pH < 5.0$) the Al_{13}-mer is active. For $pH > 4.5$, the contribution of K^I to eqn (8) is negligible (Fig. 7B). In this pH range, $\log[K_{app}/(_{LAl}{}^{13})]$ *versus* pH plots at different C_M (Fig. S5 A, ESI), and $\log[K_{app}[H^+]^{32}/(_{LAl}{}^{13})]$ *versus* C_M plot (Fig. S5 B, ESI)

yielded straight lines with slope equal to 32 and 12, respectively, reinforcing the presence of $Al_{13}O_4(OH)_{24}^{7+}$ as the reactive species. Analysis according to eqn (8) of K_{app} *versus* pH plots yielded $K^{VIII} = (1.6 \pm 0.4) \times 10^6\ M^{-12}$ (Fig. 7B). This datum can be used in the $3.0 < pH < 4.3$ region to evaluate $K^{I} = (4 \pm 2) \times 10^4\ M^{-1}$.

Also, from the NMR data obtained we evaluated the apparent equilibrium constant at $C_L = C_M$ and different pH values (see ESI). The K_{app} values obtained at pH values 4 and 5 (Table 1 ESI) concur well with the spectrophotometric values (Table 1). However, the values obtained at pH 6 and 7 are smaller than expected, thus disagreeing with the model proposed by means of UV measurements (Fig. 6 ESI) due to the observed aggregation trend of the Al_{13} units.

^{27}Al-NMR results show that the interaction between metal and ligand yield the AlCac complex and not AlHCac or AlH_2Cac, however no indication is provided as to forming AlCac from reactions (9) or (10) written below.

$$Al^{3+} + Cac^{-} = AlCac^{2+} \qquad (9)$$

Due to the proton ambiguity, reaction (9) cannot be thermodynamically distinguished from the equivalent reaction (10)

$$AlOH^{2+} + HCac = AlCac^{2+} \qquad (10)$$

Being $AlOH^{2+}$ about 10^4-fold more reactive than Al^{3+} aquo ion, as results from comparison of the respective rates of water exchange [REF Nordin JP, Sullivan DJ et al. Inorg Chem 1998 37(19) 4760-4763 An 17O-NMR study of the exchange…] the

first step of the Al(III) binding to a chelating ligand should be about 10^3-fold faster in the case of $AlOH^{2+}$.[REF Secco venturini Inorg. Chem. 1975 Mechanism of Complex formation.Reaction between Aluminum and Salycilate ions] Hence, for pH > 2 the formation of $AlCac^{2+}$ will undergo mainly through reaction (10). The equilibrium constant of reaction (10), here denoted as K^{I}', is related to K^{I} by the relationship $K^{I}' = K^{I}K_{A2}/Q_{11}$. Its value is $K^{I}' = (8 \ \ 4) \times 10^3\ M^{-1}$. Only for pH > 5 the contribution of the deprotonated Cac^- ion to the binding reaction becomes important. This interpretation differs from that advanced in a previous study were the formation of the 1:1 complex was rationalized assuming that the main process is the reaction of the Al^{3+} ion with the deprotonated form of the ligand, Cac^-.[19]

DFT calculations: hypothesis of Al/Cac structures. By means of the mass spectrometry and NMR data, we have hypothesized possible Al/Cac structures. It can reasonably be assumed that the ligand chelates the metal, as demonstrated for other oxygenated ligands with aluminium.[26,41,42]

The suggested structure of the monomer species is shown in Fig. 8A (note that water molecules can be replaced by hydroxo groups, and more than one ligand could be present). For the dimer species, the mass spectrometry and NMR data gathered do not clarify the exact structure, so different geometries can be considered. Based on earlier studies on different Al(III) complexes,[31,41] we propose the following structures: two aluminium atoms linked by two oxygen groups (Fig. 8B), the interaction of the aluminium complexes is obtained via hydroxo groups (Fig. 8C), only one oxygen binds the aluminium complexes, as in the third structure (Fig. 8D). Interestingly, a different M_2L structure is proposed for the aluminium/acetate complex.[41] Since cacodylate

exhibits similar structure as the acetate, we proposed similar geometry associated to the most intense signal in the mass spectrometry (m/z = 121) and NMR spectra (δ = 1.95 and 1.80 ppm) (Fig. 8E). As a matter of fact, a *syn-syn* bridging geometry is considered by the experimental results, where the two oxygens bind to both aluminium atoms of the dimeric form. Hence, a double hydroxo- or oxo- bridged geometry is present. For the trimeric and tetrameric species, other more complex structures can be hypothesized with the same bridging geometry.

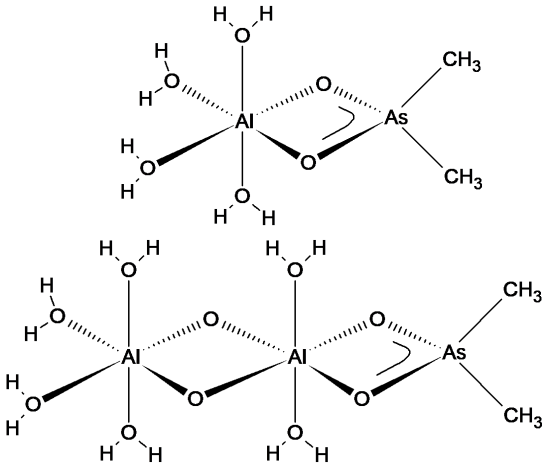

A

B

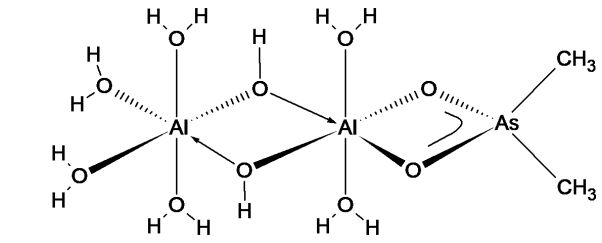

C

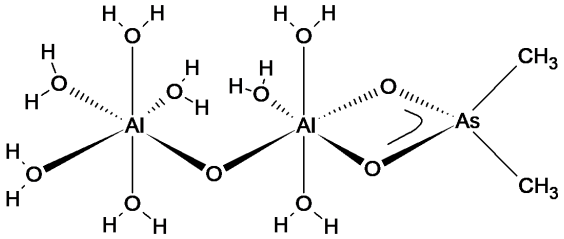

D

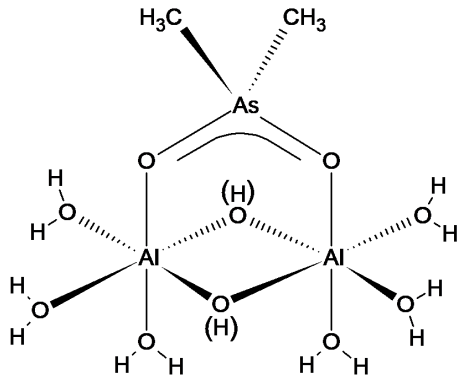

E

Fig. 8 (A) 1:1 structure. (B) First 2:1 structure. (C) Second 2:1 structure, (D) Third 2:1 structure (E) Fourth 2:1 structure: *syn-syn* bridging geometry.

To convincingly justify the hypotheses drawn on the dimeric complexes, we undertook theoretical energy calculations of these complexes.

For the M_2L dimeric system, four different structures were calculated (B,C and two more E structures, with and without bridging oxygens, which will be denoted as E(OH) and E(O), respectively. The two E structures consist of a 2:1 complex, where Cacodylate is bound to only one Al atom via a double O-bridge. B and C structures resemble the E(O) and E(OH) structures, respectively, but with OH bridging ligands between Al atoms, instead of O-bridge, and two more hydroxo ligands.

The stability has been studied in terms of the overall energy (products energy). The DFT optimization of these structures results in the stability sequence, from most stable to less stable (Hartree units), as follows: (B) (-849.660435) > (C) (-849.651503)> (E(O)) (-849.590124) > (E(OH)) (-849.558751). Thus, the most stable structure involves OH-bridging ligands between Al atoms with cacodylate bound to both metal centres. The optimized structure of (E(OH) is plotted in Fig. 9A.

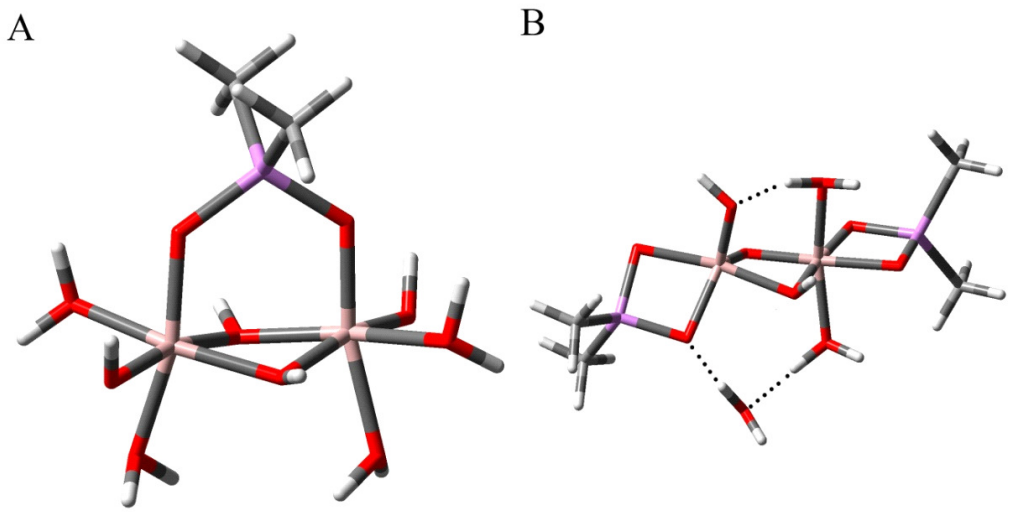

Fig. 9 (A) DFT optimization of structure E(OH) in water, using B3LYP functional with 6-31G(d) basis set for C (grey), H (white) and O (red) atoms, and LANL2DZ for Al (pink) and As (purple) atoms. (B) DFT optimization of 2:2 linear complex in water, using B3LYP functional with 6-31G(d) basis set for C(grey), H(white) and O(red) atoms, and LANL2DZ for Al (pink), As (purple) atoms and H-bonding interactions (dashed lines).

A non-symmetrical conformation has been obtained (symmetry group C1) with OH groups in the Al-Al plane pointing to cacodylate group. Surprisingly, methyl groups bound to As, adopted eclipsed conformation. Full NBO (Natural Bond Orbital) analysis has revealed that, as expected, the Al and As sites are mainly positively

charged. Oxygen atoms in the Al-O-As bonds are significantly more negative than the others due to the charge donating nature of the metals. Thus, the Oxygen site in the OH-bridges between Al atoms are, indeed, more negative than those on the water molecules.

The characterization parameters (bond distance and angle) of the "core" of the molecule (every atom surrounding Al and As atoms) are compiled in Table S2, ESI. The two atom distances and angles containing Al are similar, showing that the core lies in a symmetric environment and the abovementioned asymmetry is due to the slightly asymmetric conformation of the H_2O, OH and CH_3 groups.

In addition, DFT optimization and geometry analysis of two 2:2 complex (structures reported in Fig. S7, ESI), has been carried out, whose presence was confirmed by mass spectrometry (m/z = 361). Since the calculations of a double *syn-syn* bridging geometry complex (Fig. S7 A, ESI) proved to be unstable in water, complex linear geometry (Fig. S7 B, ESI) has been DFT optimized to a minimum energy state (E= -933.31Hartrees). In the final conformation, one hydrogen atom from a water molecule is lost, and transferred to one of the O-bridging ligand between Al atoms. Moreover, a full water molecule is lost, remaining nearby the 2:2 complex via H-bonding interaction (Fig. 9B). These rearrangements, result in a surprisingly different conformation for Al atoms, from the initial Al(octhedral)-Al(octahedral) to Al(pyramidal)-Al(octahedral). The stabilization of the pyramidal configuration can be explained by the H-bonding induced by the above mentioned water molecule that falls off the molecule (Table S3, ESI), showing that expected symmetry of the optimized structure is totally lost. The distance and angle values of the Al-O bonds considerably differ from their theoretical mirror image bonds. The dihedral angles show different

orientation of the As-O-Al(pyramidal)-O and As-O-Al(octahedral) rings compared to the plane containing Al(1), O(2) and Al(3); the Al(pyramidal) ring is primarily orientated to the yz plane, whereas the Al(octahedral) containing ring, lies in the xz plane. As described for the 2:1 complex, the NBO analysis displays electron donation from metals to oxygen, an effect more intense for the O-bridging ligands between Al atoms.

4. Conclusion

Thermodynamic experiments of the interaction between Al(III) and dimethylarsinic acid suggest that the apparent binding affinity has a maximum in the 5-6 pH region, whereas at pH 4 and pH 7 the binding strength is low. Comparison of the MS and NMR data suggests that the main species formed is a 2:1 complex. Thus, the most probable effect is that the 1:1 complex, which forms first, has a high affinity for a second aluminium ion. In particular, the most plausible structure is the dimeric *syn-syn* bridging geometry structure of the cacodylate, interacting with the two aluminium centres (Fig. 8E). On the other hand, the different behaviour observed at pH 7 respect to that at pH 4-6 is explained assuming the formation of an outer sphere coordination of the ligand to the Al_{13} aggregates at neutral pH, thus avoiding precipitation. On the other hand, at lower pH the polymeric form disintegrates into small molecules, an effect promoted mainly by the proton and, to a less extent, by the ligand. Elucidation of the Al/Cac complex, which does not allow aluminium to precipitate, can be very useful to obtain a system available to study the biological processes and molecular mechanisms that underlie pathological effects induced by aluminium ions.

Acknowledgements

This work was supported by Obra Social "la Caixa" (OSLC-2012- 007), and MINECO, CTQ2014-58812-C2-2-R projects, Spain

Notes and References

1. C. F. Baes and R. E. Mesmer, in *Hydrolysis of Cations*, John Wiley & Sons, New York1976, ch. 6, pp. 112-123.
2. M. Lamberti, I. D'Auria, M. Mazzeo, S. Milione, V. Bertolasi and D. Pappalardo, *Organometallics*, 2012, **31**, 5551-5560.
3. J. I. Mujika, J. M. Ugalde and X. Lopez, *Phys. Chem. Chem. Phys.*, 2012, **14**, 12465-12475.
4. S. Bhattacharjee, Y. Zhao, J. M. Hill, F. Culicchia, T. P. A. Kruck, M. E. Percy, A. I. Pogue, J. R. Walton and W. J. Lukiw, *J. Inorg. Biochem.*, 2013, **126**, 35-37.
5. T. Kiss, *J. Inorg. Biochem.*, 2013, **128**, 156-163.
6. A. Strunecka, R. L. Blaylock and J. Patocka, *Curr. Inorg. Chem.*, 2012, **2**, 8-18.
7. C. Exley and J. D. Birchall, *J. Theor. Biol.*, 1992, **159**, 83-98.
8. E. H. Jeffery, K. Abreo, E. Burgess, J. Cannata and J. L. Greger, *J. Toxicol. Env. Health*, 1996, **48**, 649-665.
9. S. A. Latt and H. A. Sober, *Biochemistry*, 1967, **6**, 3307-3314.
10. B. Holmberg., *Z. Phys. Chem.*, 1910, **70**, 153-158.
11. J. Juillard and N. Simonet, *Bull. Soc. Chim. Fr.*, 1968, 1883-1894.
12. K. B. Jacobson, B. D. Sarma and J. B. Murphy, *FEBS Lett.*, 1972, **22**, 80-82.
13. T. W. Shin, K. Kim and I. J. Lee, *J. Solution Chem.*, 1997, **26**, 379-390.
14. H. Diebler, F. Secco and M. Venturini, *Biophys. Chem.*, 1987, **26**, 193-205.
15. P. V. Ioannou, *Monatsh. Chem.*, 2012, **143**, 1349-1356.
16. P. V. Ioannou, *Z. Anorg. Allg. Chem.*, 2010, **636**, 1347-1353.
17. C. F. Whittemore and C. James, *J. Am. Chem. Soc.*, 1913, **35**, 127-132.
18. R. Pietsch, *Microchim. Acta*, 1958, 220-224.
19. P. V. Ioannou, *Monatsh. Chem.*, 2013, **144**, 793-802.
20. M. Lashkari and M. R. Arshadi, *Chemical Physics*, 2004, **299**, 131-137.
21. M. J. Frisch, G. W. Trucks, H. B. Schlegel, G. E. Scuseria, M. A. Robb, J. R. Cheeseman, G. Scalmani, V. Barone, B. Mennucci, G. A. Petersson, H. Nakatsuji, M. Caricato, X. Li, H. P. Hratchian, A. F. Izmaylov, J. Bloino, G. Zheng, J. L. Sonnenberg, M. Hada, M. Ehara, K. Toyota, R. Fukuda, J. Hasegawa, M. Ishida, T. Nakajima, Y. Honda, O. Kitao, H. Nakai, T. Vreven, J. A. Montgomery, J. E. Peralta, F. Ogliaro, M. Bearpark, J. J. Heyd, E. Brothers, K. N. Kudin, V. N. Staroverov, R. Kobayashi, J. Normand, K. Raghavachari, A. Rendell, J. C. Burant, S. S. Iyengar, J. Tomasi, M. Cossi, N. Rega, J. M. Millam, M. Klene, J. E. Knox, J. B. Cross, V. Bakken, C. Adamo, J. Jaramillo, R. Gomperts, R. E. Stratmann, O. Yazyev, A. J. Austin, R. Cammi, C. Pomelli, J. W. Ochterski, R. L. Martin, K. Morokuma, V. G. Zakrzewski, G. A. Voth, P. Salvador, J. J. Dannenberg, S. Dapprich, A. D. Daniels, Farkas, J. B. Foresman, J. V. Ortiz, J. Cioslowski and D. J. Fox, Gaussian, Inc., Revision B.01 edn., 2009.

22. K. Yates and H. Wai, *J. Am. Chem. Soc.*, 1964, **86**, 5408-5413.
23. M. L. Kilpatrick, *J. Am. Chem. Soc.*, 1949, **71**, 2607-2610.
24. G. Furrer, C. Ludwig and P. W. Schindler, *J. Colloid Interf. Sci.*, 1992, **149**, 56-67.
25. C. Ye, Z. Bi and D. Wang, *Colloids and Surfaces A*, 2013, **436**, 782-786.
26. W. H. Casey, *Chem. Rev.*, 2006, **106**, 1-16.
27. J. W. Eaton, D. Bateman and S. Hauberg, in *A High-Level Interactive Language for Numerical Computations*, Create Space Independent Publishing Platform, 3.0.1 edn., 2009.
28. M. H. Florencio, M. F. Duarte, A. M. M. deBettencourt, M. L. Gomes and L. F. V. Boas, *Rapid Commun. Mass Sp.*, 1997, **11**, 469-473.
29. H. R. Hansen, A. Raab and J. Feldmann, *J. Anal. Atom. Spectrom.*, 2003, **18**, 474-479.
30. T. Urabe, M. Tanaka, S. Kumakura and T. Tsugoshi, *J. Mass Spectrom.*, 2007, **42**, 591-597.
31. A. Sarpola, V. Hietapelto, J. Jalonen, J. Jokela and R. S. Laitinen, *J. Mass Spectrom.*, 2004, **39**, 423-430.
32. A. T. Sarpola, V. K. Hietapelto, J. E. Jalonen, J. Jokela and J. H. Ramo, *Int. J. Environ. An. Ch.*, 2006, **86**, 1007-1018.
33. A. Sarpola, V. Hietapelto, J. Jalonen, J. Jokela, R. S. Laitinen and J. Ramo, *J. Mass Spectrom.*, 2004, **39**, 1209-1218.
34. T. Urabe, T. Tsugoshi and W. Tanakaa, *J. Mass Spectrom.*, 2009, **44**, 193-202.
35. J. W. Akitt and B. E. Mann, *J. Magn. Reson.*, 1981, **44**, 584-589.
36. J. J. Fitzgerald, L. E. Johnson and J. S. Frye, *J. Magn. Reson.*, 1989, **84**, 121-133.
37. G. Furrer, M. Gfeller and B. Wehrli, *Geochim. Cosmochim. Acta*, 1999, **63**, 3069-3076.
38. A. Masion, F. Thomas, D. Tchoubar, J. Y. Bottero and P. Tekely, *Langmuir*, 1994, **10**, 4353-4356.
39. A. Amirbahman, M. Gfeller and G. Furrer, *Geochim. Cosmochim. Acta*, 2000, **64**, 911-919.
40. W. Stumm, in *Chemistry of the solid-water interface: processes at the mineral-water and particle-water interface in natural systems*, John Wiley & Sons, New York1992, ch. 1, pp. 4-8.
41. P. Persson, M. Karlsson and L. O. Ohman, *Geochim. Cosmochim. Acta*, 1998, **62**, 3657-3668.
42. R. B. Martin, *Clin. Chem.*, 1986, **32**, 1797-1806.